

# Combined population and evolutionary synthesis of galaxy spectra

A. Goerdt and W. Kollatschny

Universitäts-Sternwarte Göttingen, Geismarlandstraße 11, D-37083 Göttingen, Germany

Received 29 January 1998 / Accepted 26 June 1998

**Abstract.** We present our numerical code to perform syntheses of galaxy spectra. Our modified linear simplex algorithm has the advantage that no initial solution is required, the non-negativity for the individual contributions is guaranteed, additional spectral components can be added and individual wavelength regions can be weighted. Synthesizing the observed galaxy spectra with isochrone spectra we determine the age distribution of the stellar component. We demonstrate the accuracy of our method to reconstruct the age distribution of theoretical spectra. Finally, we present evolutionary syntheses of the optical spectra of an elliptical galaxy and of the spatially resolved Seyfert galaxy NGC 1365.

**Key words:** galaxies: stellar content – galaxies: evolution – galaxies: individual: NGC 1365 – galaxies: Seyfert

## 1. Introduction

During the last years great effort has been made to determine the stellar population and their age distribution in galaxies. These population synthesis models depend mainly on the numerical methods to optimize the spectral fittings and on the stellar libraries used for the synthesis. If one is interested in the age distribution of the stellar component one can perform evolutionary syntheses using stellar evolutionary tracks. Important papers on these subjects have been published by Arimoto & Yoshii (1987), Bica & Alloin (1986), Bruzual (1983), Guiderdoni & Rocca-Volmerange (1987), O’Connell (1976), Pelat (1997), Pickles & van der Kruit (1990) etc. These authors use different mathematical methods for their syntheses.

We are especially interested in the spectral synthesis of AGN spectra. If active galactic nuclei are triggered by tidal forces we expect a different stellar composition in their host galaxies in comparison to normal galaxies. Therefore, further spectral components (e.g. a non-thermal component) have to be considered in addition to extinction by dust. We have developed a modified simplex algorithm to perform population and evolutionary syntheses of these spectra.

*Send offprint requests to:* W. Kollatschny

First results of our program have been presented in Goerdt & Kollatschny (1996) as well as in Kollatschny & Goerdt (1997, 1998). Furthermore, a comparison of worldwide used synthesis models (including ours) of selected elliptical galaxies has been published by Arimoto (1996).

## 2. Synthesis procedure

Our problem is to determine the stellar content including star formation history of an observed galaxy spectrum. We need an automatic fitting routine which reproduces the spectral energy distribution of our observed spectrum. Thus a set of library spectra has to be combined by a mathematical formalism minimizing the differences between the observed and our composite spectrum. We employ a linear programming algorithm to minimize the mean absolute fractional residual. Using this method the non-negative constraint for the various contributions is easily guaranteed and no guess or initial solution is required to start the procedure with. Quadratic programming is quite complex and does not appear to provide any definite advantage over the method adopted here. The linear programming algorithm iterates towards the unique optimal solution (e.g. O’Connell 1976). Having  $m$  library spectra and an observed spectrum with  $n$  wavelength points our problem can be stated as

$$y_i = \sum_{j=1}^m f_{ij} x_j \quad (1)$$

$$r_i = |1 - y_i/z_i| \quad (2)$$

$$q = \sum_{i=1}^{n-1} w_i r_i \quad (3)$$

$$\epsilon = q / \sum_{i=1}^{n-1} w_i \quad (4)$$

where :

- $y_i$  : normalized flux at  $\lambda_i$  produced by the model
- $f_{ij}$  : normalized flux at  $\lambda_i$  from the  $j$ th library spectrum
- $x_j$  : fraction of light at  $\lambda_n$
- $z_i$  : normalized flux of our obs. spectrum to be analyzed
- $r_i$  : absolute value of the fractional residual between the model and the observed spectrum

$w_i$  : weighing factor assigned to the  $i$ th wavelength

$q$  : value to be minimized

$\epsilon$  : mean absolute deviation

We are interested in the  $x_j \geq 0$  ( $j = 1 \dots m$ ) in the case that  $q$  in Eq. 3 is a minimum and none of the following equations has been ignored:

$$\sum_{j=1}^{n-1} \frac{f_{ij}}{z_i} x_j + r_i \geq 1$$

$$\sum_{j=1}^{n-1} \frac{f_{ij}}{z_i} x_j - r_i \leq 1 \quad (i = 1 \dots n-1) \quad (5)$$

$$\sum_{j=1}^m x_j = 1 \quad (6)$$

$$\sum_{j=1}^m c_{ij} x_j \leq b_i \quad (i = 1 \dots k) \quad (7)$$

Eq. 5 is the equivalence to Eq. 2 and Eq. 6 expresses normalization at  $\lambda_i$  which is the  $n$ -th constraint. Additional constraints can be easily implemented regarding astrophysical constraints as a smooth mass or luminosity function of the composite spectrum (Eq. 7). To solve this problem we use a modified Simplex algorithm. First we will mention the general linear programming problem which is described in detail in Hadley (1962) before we will formulate the modifications necessary to use it for our specific task.

### 2.1. General linear programming technique

The general linear programming problem is to find a set of  $r$  variables  $x_j$   $j=1, \dots, m$  satisfying  $m$  linear constraints. These constraints are given in a form of inequalities or equalities

$$a_{i1}x_1 + \dots + a_{im}x_m \{ \geq = \leq \} b_i \quad i = 1, \dots, n \quad (8)$$

where one and only one of the signs  $\geq, =, \leq$  holds for each constraint but the sign can vary from one constraint to another. Furthermore, the variables  $x_j \geq 0$   $j = 1, \dots, m$  are restricted to be non-negative. The expression

$$z = c_1x_1 + \dots + c_mx_m \quad (9)$$

has to be maximized or minimized. All  $a_{ij}, b_i, c_j$  are assumed to be known constants.

Any set of  $x_j$  which satisfies the set of constraints and maximizes or minimizes the values of  $z$  in Eq. 9 is called a feasible solution. There is no way to find the optimal feasible solution instantaneously. Otherwise, to compare all feasible solutions to be optimal is much effort: the number of the basic feasible solutions (the optimal feasible solution is one of them) increases by  $\frac{m!}{n!n!}$  where  $m$  is the number of variables and  $n$  the number of constraints. To achieve a set of equalities instead of inequalities written in matrix form  $Ax = b$ , all inequalities in Eq. 8 have to be converted into equalities.

Consider first the  $\leq$  sign: this constraint - we call it  $h$  - can be written as

$$\sum_{j=1}^m a_{hj}x_j \leq b_h \quad (10)$$

We introduce a new variable  $x_{m+h} \geq 0$  by

$$x_{m+h} = b_h - \sum_{j=1}^m a_{hj}x_j \quad (11)$$

Then Eq. 10 can be rewritten as

$$\sum_{j=1}^m a_{hj}x_j + x_{m+h} = b_h \quad (12)$$

Next consider the  $\geq$  sign - the notation will be  $k$  - and we will eventually get:

$$\sum_{j=1}^m a_{kj}x_j - x_{m+k} = b_k \quad (13)$$

The variables  $x_{m+h}$  and  $x_{m+k}$  are called slack and surplus variables.

Thus we have converted all inequalities in Eq. 8 into equalities. For every inequality we have obtained a new variable. Originally having  $v$  inequalities out of  $n$  constraints containing  $m$  variables we will finally have  $m + v = r$  variables.

The set of equations can now be written in matrix form as

$$Ax = x_1a_1 + \dots + x_ra_r = b \quad (14)$$

Despite of adding new variables the function to optimize does not change. Originally, we had

$$z = \sum_{j=1}^m c_jx_j \quad (15)$$

If we assign all  $c_j = 0$  associated to the slack and surplus variables  $x_j$  the value of  $z$  is not affected by conversion of the constraints to a system of simultaneous equations:

$$\begin{aligned} \sum_{j=1}^r c_jx_j &= c_1x_1 + \dots + c_mx_m + 0x_{m+1} + \dots + 0x_{m+v} \\ &= \sum_{j=1}^m c_jx_j \end{aligned} \quad (16)$$

To solve this problem it is necessary that there are at least as many variables as constraints. The rank of the matrix  $A$  remains the same although  $A$  has been augmented by the slack and surplus variables

$$r(A) \leq n \quad (17)$$

where  $n$  is the number of constraints. If the number of variables is the same as the number of equations there is only one optimal feasible solution (if there is a feasible solution at all).

If  $Ax = b$  and  $r(A) = n$ , then  $b$  can be written as a linear combination of  $n$  linear independent columns in matrix  $A$ . Thus we yield a solution with no more than  $n$  variables not equal zero. These solutions are called basic solutions. Now our system of linear equations is reduced to  $Bx_B = b$ ,  $B$  is a quadratic  $n \times n$  matrix and part of  $A$ . The  $x_B$  are the basic non-zero variables giving a solution. Our function to optimize shortens to

$$z = c_B x_B \quad (18)$$

since all non basic (non-zero) variables vanish.

Now, every vector (column) of  $A$  can be written as a linear combination of the columns of  $B$  (basic vectors)

$$a_j = \sum_{i=1}^n y_{ij} b_i \quad (19)$$

Let us remove the  $r$ -th column of  $B$   $b_r$  and replace it with the  $j$ -th column of  $A$   $a_j$  which is not already part of  $B$

$$b_r = \frac{1}{y_{rj}} a_j - \sum_{\substack{i=1 \\ i \neq r}}^m \frac{y_{ij}}{y_{rj}} b_i \quad (20)$$

Inserting Eq.20 into Eq.19 a different solution can be written as

$$\sum_{\substack{i=1 \\ i \neq r}}^m \left( \underbrace{x_{Bi}}_{\hat{x}_{Bi}} - x_{Br} \frac{y_{ij}}{y_{rj}} \right) b_i + \underbrace{\frac{x_{Br}}{y_{rj}}}_{\hat{x}_{Br}} a_j = b \quad (21)$$

The  $\hat{x}_{bi}$  are the new basic variables with the new vector  $x_k$  instead of vector  $x_r$ .

The changing of matrix  $A$  by replacing column  $b_r$  with  $a_k$  is given in the following equations

$$a_j = \sum_{i=1}^m y_{ij} b_i \quad (22)$$

$$b_r = - \sum_{\substack{i=1 \\ i \neq r}}^m \frac{y_{ik}}{y_{rk}} b_i + \frac{1}{y_{rk}} a_k \quad (23)$$

$b_r$  inserted in Eq. 22 gives

$$\begin{aligned} a_j &= \sum_{\substack{i=1 \\ i \neq r}}^m \left( y_{ij} - y_{ri} \frac{y_{ik}}{y_{rk}} \right) b_i + \frac{y_{rj}}{y_{rk}} a_k \\ &= \sum_{i=1}^m \hat{y}_{ij} b_i \end{aligned} \quad (24)$$

where

$$\hat{y}_{ij} = y_{ij} - y_{rj} \frac{y_{ik}}{y_{rk}} \quad i \neq r \quad (25)$$

$$\hat{y}_{ij} = \frac{y_{rj}}{y_{rk}} \quad i = r \quad (26)$$

Our new value  $z$  can be obtained by exchanging the basic vectors

$$\hat{z} = \sum_{\substack{i=1 \\ i \neq r}}^m c_{Bi} \left( x_{Bi} - x_{Br} \frac{y_{ij}}{y_{rj}} \right) + \frac{x_{Br}}{y_{rj}} c_j \quad (27)$$

For  $i = r$  there is

$$c_{Bi} \left( x_{Br} - x_{Br} \frac{y_{rj}}{y_{rj}} \right) = 0 \quad (28)$$

Hence Eq. 27 can be rewritten as

$$\hat{z} = \sum_{i=1}^m c_{Bi} \left( x_{Bi} - x_{Br} \frac{y_{ij}}{y_{rj}} \right) + \frac{x_{Br}}{y_{rj}} c_j \quad (29)$$

$$\hat{z} = \sum_{i=1}^m c_{Bi} x_{Bi} - \frac{x_{Br}}{y_{rj}} \sum_{i=1}^m c_{Bi} y_{ij} + \frac{x_{Br}}{y_{rj}} c_j \quad (30)$$

$$\hat{z} = z + \frac{x_{Br}}{y_{rj}} (c_j - z_j) \quad (31)$$

$$\hat{z} = z + \theta (c_j - z_j) \quad (32)$$

where

$$z_j = \sum_{i=1}^m c_{Bi} y_{ij} \quad (33)$$

and

$$\theta = \frac{x_{Br}}{y_{rj}} \quad (34)$$

Having a maximization problem  $\hat{z}$  will increase if the following conditions are true

- i)  $\theta > 0$
- ii)  $(c_j - z_j) > 0$

By minimizing  $z$  one of the arguments must not be negative. Checking the validity of these conditions can be done without much computing effort. To make clear the sequence of iteration: first we try to find out which vector would give an improved  $z$  by testing both conditions. After being verified we exchange the vectors to gain the new calculated  $z$  and start to check (i) and (ii) again. This process of iteration terminates in either way:

- a) One or more  $z_j - c_j < 0$  for all  $y_{ij} \leq 0$
- b) All  $z_j - c_j \geq 0$  for all columns in  $A$  which are not part of  $B$ .

In case a there is only an unbounded solution; case b turns out to be the optimal feasible solution (Hadley 1962).

## 2.2. Modified simplex algorithm

The general simplex algorithm technique cannot be applied to our problem in the way described above. The ordinary simplex algorithm means maximization of a negative value when speaking about a minimization problem. In that case the spectral energy distribution of our synthesized spectrum would be completely below or above the observed spectrum at every wavelength point. All deviations at every wavelength point between the observed and the synthesized spectrum would be either negative or positive.

For our problem it is essential that at every arbitrary wavelength point the flux of the calculated synthesized spectrum can be less, equal or more than the observed flux. This means that we have to minimize the absolute residuals. In matrix form our problem can be written as:

$$Sx = b \quad (35)$$

Each column of  $S$  is one spectrum of the stellar library. The vector  $b$  is the spectrum to be analyzed. The problem is how to combine the stellar spectra to achieve an almost identical spectrum of  $b$  and to determine the  $x_j$ .

$S$  is a  $n \times m$  matrix where  $n$  is the number of wavelength points and  $m$  the number of spectra in our stellar library. It is very improbable that one finds a solution satisfying all constraints the equal sign being valid. This means we have a set of  $(n - 1)$ -inequalities and an equation that satisfies Eq. 6 due to normalization at wavelength  $\lambda_n$ . All inequalities have to be converted into equalities. But we do not know in advance whether or not there will be a positive or negative deviation to our optimal fit. A pair of one slack and one surplus variable must be introduced for each constraint respectively wavelength point  $i, i = 1, \dots, n - 1$ . Then our new set contains  $2 \times (n - 1)$  new variables which stand for the differences in flux between the observed and the computed energy distribution. Anyway, either new variable of each pair will be zero. Both variables are zero in case the equal sign fits.

Now we have an equation in matrix form  $Ax=b$  where  $A$  is a  $n \times (m + 2n)$  matrix. The slack and surplus variables  $x_j, j = m + 1, \dots, 2(n - 1)$  are to be minimized.

$$z = \sum_{j=m+1}^{m+2(n-1)} c_j x_j \quad (36)$$

Now recall the initial statement of our problem and compare it with our results: the  $x_j$  correspond to the differences  $r_i = |1 - y_i/z_i|$  in Eq. 2. The  $c_j$  are the weighing factors  $w_i$  and  $z$  corresponds to  $q$  in Eq. 3. The quality of our fit in other words the mean deviation is given by

$$\epsilon = z / \sum_{j=1}^{n-1} c_j \quad (37)$$

Consider Eqs. 30 to 33:  $\hat{z}$  is lower than the previous value of  $z$  if  $(c_j - z_j) < 0$  and  $\theta = \frac{x_{Br}}{y_{rk}} > 0$ . The possibility with reversed signs contradicts the constraint  $\theta < 0$ ;  $\theta$  is the new basic variable  $\hat{x}_{Br}$  (Eq. 21) which must be non-negative.

If an optimal feasible solution has been found  $z$  has been minimized. The  $x_j$  are the fractions of light of the  $m$  library stars reproducing the observed spectral energy distribution  $b$ . The fractions of light are the light contributions at the normalized wavelength  $\lambda_n$ .

### 3. Stellar libraries

To analyse the stellar population in galaxy spectra one needs a comprehensive reference stellar library. The spectra of the library should cover a sufficient large wavelength range and they should be comparable in spectral resolution in comparison to the observed galaxy spectra. Furthermore, the stellar library should be as complete as possible. This means all spectral components the galaxy consists of should be included in the library. Presently we can choose between four stellar libraries for the synthesis of galaxy spectra and for the construction of individual isochrones: three libraries of observed stellar spectra mostly

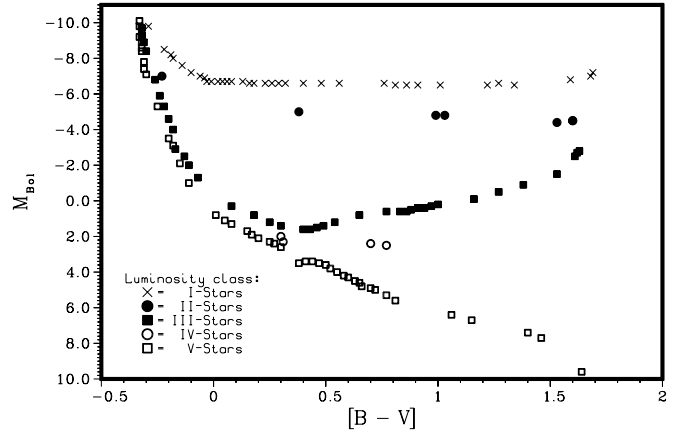


**Fig. 1.** All stars contained in the stellar library of Jacoby, Hunter & Christian are shown in this colour-magnitude diagram

with solar metallicities: Gunn & Stryker (1983), Jacoby, Hunter & Christian (1984) and Silva & Cornell (1992) and a homogeneous sample of model atmospheres with various metallicities calculated by Kurucz (1994).

#### 3.1. Gunn & Stryker library

The stellar library of Gunn & Stryker (1983) consists of 175 observed spectra mostly with solar metallicity. The spectra cover a large spectral range from  $\lambda = 3180 \text{ \AA}$  until  $\lambda = 10620 \text{ \AA}$ . On the other hand the spectral resolution of  $20 \text{ \AA}$  in the blue and of  $40 \text{ \AA}$  in the red range is not very high. We placed the stars at a common distance of  $r = 10 \text{ pc}$  and converted the observed fluxes into absolute magnitudes.

#### 3.2. Jacoby, Hunter & Christian library

Jacoby, Hunter & Christian (1984) observed 161 stars in the spectral range of  $3510 \text{ \AA} - 7427 \text{ \AA}$  at sufficient spectral resolution ( $\sim 4.5 \text{ \AA}$ ). The library data are given as  $F(\lambda)$  over  $\lambda$ . Again we calculate the flux  $F_{abs}(\lambda)$  for a distance of  $10 \text{ pc}$ . The  $m_V$  of all library stars are given too by Jacoby, Hunter & Christian (1984). For an overall view we plotted the positions of all stars contained in the Jacoby, Hunter & Christian library in the colour-magnitude diagram in Fig. 1.

#### 3.3. Silva & Cornell library

Silva & Cornell (1992) published the optical spectra of a stellar library containing 72 objects. Most of them have an atmosphere with solar metallicity; additionally, a few of them are either metal-poor or metal-rich. The spectra extend from  $3510 \text{ \AA} - 8930 \text{ \AA}$  at a resolution of  $\sim 11 \text{ \AA}$ .

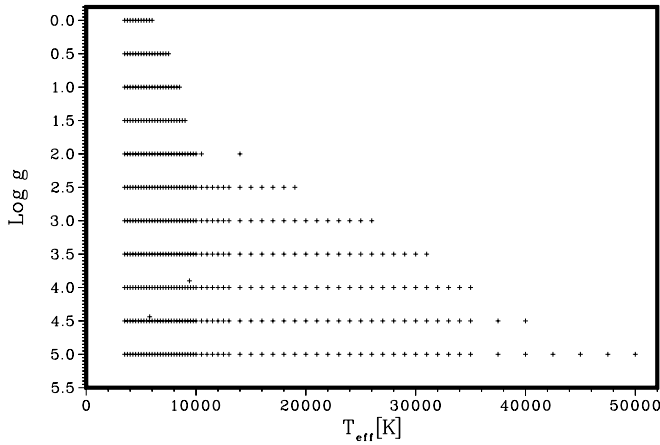


**Fig. 2.**  $T_{eff}$  and  $\log g$  values in the grid of stellar atmospheres of Kurucz

### 3.4. Kurucz library

Kurucz (1992,1994) published the most comprehensive library of synthetic stellar spectra existing so far. He calculated a grid of 7619 model atmospheres for scaled solar abundances between  $[-5.0]$  and  $[+1.0]$ . The spectra extend from  $90.9 \text{ \AA} - 160 \text{ \mu m}$ . A spectrum consists of 1221 wavelength steps; this corresponds to a spectral resolution of  $20 - 40 \text{ \AA}$  in the optical. He calculated his grid of model atmospheres for temperatures in the range between  $T_{eff} = 3500 \text{ K}$  and  $50.000 \text{ K}$  in steps of  $250 \text{ K}$  and for  $\log g$  values of  $0.0 \leq \log g \leq 5.0 \frac{m}{s^2}$  in steps of  $0.5$ . The grid of models for solar metallicity is plotted in Fig. 2.

### 3.5. Additional spectral components

The continuum emission of galaxies - especially that of active galactic nuclei - is not only composed of individual stellar continua. There might be an additional central, non-thermal continuum component of importance and possibly a Balmer continuum and/or a quasi continuum of blended FeII lines.

#### 3.5.1. Non-thermal continuum component

The spectra of the central regions of active galaxies might be dominated by a nuclear non-thermal emission. If one carries out syntheses of central galaxy regions this component has to be considered therefore. The spectral flux distribution of this component can be described in a first order approximation by

$$F(\nu) \sim \nu^{-\alpha} \quad (38)$$

or

$$F(\lambda) \sim \lambda^{(\alpha-2)} \quad (39)$$

in the optical. The non-thermal continuum components of Liners, Seyfert galaxies and quasars have a typical intrinsic spectral index  $\alpha$  between  $0.7$  and  $1.5$ .

Therefore, we expanded our stellar libraries by additional continuum components with spectral indexes  $\alpha$  of  $0.7$  to  $1.6$ .

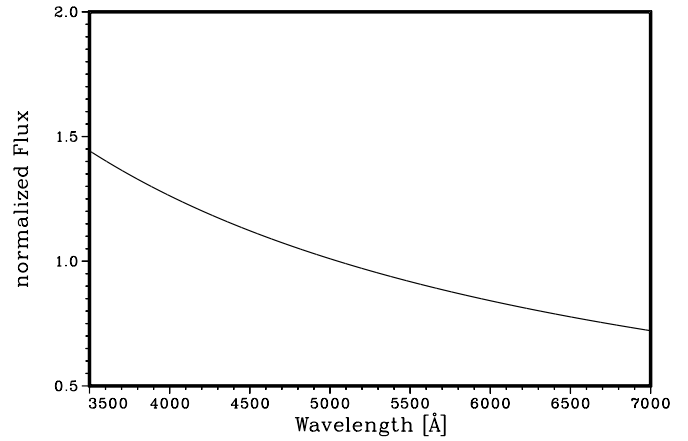


**Fig. 3.** Spectral energy distribution of a non-thermal component with spectral index  $\alpha = 1$

This central component originating in the innermost galaxy regions might be reddened by dust. Furthermore, this reddening might be different (stronger) in comparison to the galactic absorption only. We consider this effect in the way that we carry out our spectral synthesis with independent reddening for the central non-thermal components and for the galactic absorption components.

We show in Fig. 3 the spectral energy distribution of a non-thermal component with spectral index  $\alpha = 1$  without any additional absorption. The intensity has been normalized at  $\lambda 5050 \text{ \AA}$ .

#### 3.5.2. Balmer continuum, FeII quasi continuum

The continuum component in the optical and in the near UV might be heavily contaminated by a Balmer continuum and/or a FeII quasi continuum. Therefore, these components have to be considered if one makes syntheses of AGN spectra. The FeII quasi continuum is formed by thousands of emission lines in the wavelength range between  $1200 \text{ \AA}$  and  $9000 \text{ \AA}$ . Model calculations and observations of this component as well as of the Balmer continuum have been published e.g. by Netzer & Wills (1983) and Wills et al. (1985). We added to our synthesis library these spectral energy distributions of a Balmer continuum and a FeII quasi continuum.

## 4. Isochrone spectra

The population synthesis of integrated galaxy spectra with stellar spectra gives us the individual numbers of the stars. Being interested in the evolutionary history of galaxies one has to combine stellar spectra into model spectra of specified ages. These spectra are called isochrones. Using these isochrone spectra for our synthesis procedure we will gain information about the evolutionary history of the galaxy.

A crucial point in the construction of isochrones is the accuracy of stellar evolutionary tracks, the completeness of stellar libraries as well as the method to determine the light fraction of individual stars to construct isochrone spectra. Further ingre-

**Table 1.** Time steps of isochrones [yr]

$4.0 \cdot 10^6$	$4.0 \cdot 10^7$	$4.0 \cdot 10^8$	$4.0 \cdot 10^9$	$13.2 \cdot 10^9$
$5.0 \cdot 10^6$	$5.0 \cdot 10^7$	$5.0 \cdot 10^8$	$5.0 \cdot 10^9$	$13.8 \cdot 10^9$
$6.3 \cdot 10^6$	$6.3 \cdot 10^7$	$6.3 \cdot 10^8$	$6.3 \cdot 10^9$	$14.5 \cdot 10^9$
$8.0 \cdot 10^6$	$8.0 \cdot 10^7$	$8.0 \cdot 10^8$	$8.0 \cdot 10^9$	$15.1 \cdot 10^9$
$1.0 \cdot 10^7$	$1.0 \cdot 10^8$	$1.0 \cdot 10^9$	$10.0 \cdot 10^9$	$15.9 \cdot 10^9$
$1.3 \cdot 10^7$	$1.3 \cdot 10^8$	$1.3 \cdot 10^9$	$10.5 \cdot 10^9$	$16.6 \cdot 10^9$
$1.6 \cdot 10^7$	$1.6 \cdot 10^8$	$1.6 \cdot 10^9$	$11.0 \cdot 10^9$	$17.4 \cdot 10^9$
$2.0 \cdot 10^7$	$2.0 \cdot 10^8$	$2.0 \cdot 10^9$	$11.5 \cdot 10^9$	$18.2 \cdot 10^9$
$2.5 \cdot 10^7$	$2.5 \cdot 10^8$	$2.5 \cdot 10^9$	$12.0 \cdot 10^9$	$19.1 \cdot 10^9$
$3.2 \cdot 10^7$	$3.2 \cdot 10^8$	$3.2 \cdot 10^9$	$12.6 \cdot 10^9$	$20.0 \cdot 10^9$

**Table 2.** Chemical composition of isochrones

Z	He
0.0004	0.23
0.0010	0.23
0.0040	0.24
0.0080	0.25
0.0200	0.28
0.0500	0.352

dients are the initial mass functions (IMF) of the star forming regions and possible lower and upper limits of the stellar mass spectrum.

We are using a grid of isochrones published by Bertelli et al. (1994) for the construction of our isochrone spectra. This grid is one of the most complete ones that are presently available. The ages of the isochrones correspond to the range  $4 \cdot 10^6$  to  $20 \cdot 10^9$  years. The individual time steps of the isochrones are listed in Table 1.

Bertelli et al. (1994) calculated stellar models with initial masses in the range between 0.5 and  $120 M_{\odot}$ . The stellar evolutionary tracks were calculated from the zero age main sequence to the central carbon ignition for massive stars and to the beginning of the thermally pulsing regime of the asymptotic giant branch phase for low and intermediate stars. Furthermore, isochrones going from the tip of the AGB down to the WD cooling sequence are listed. The initial chemical compositions of the isochrones range from very low to high metal content. Table 2 lists the chemical compositions of the theoretical isochrones.

#### 4.1. Synthetic isochrone spectra

In the tables of Bertelli et al. (1994) masses, temperatures, colours, luminosities etc. are given for each isochrone. For the construction of the synthetic isochrone spectra we have to combine stellar spectra from the libraries appropriate to these isochrones. First, we describe the method how to calculate isochrone spectra from observed and theoretical stellar spectra. Then we compare the synthetic isochrone spectra derived from the different libraries.

##### 4.1.1. Synthetic isochrone spectra from observed stellar libraries

We derive the  $(V - I)_C$  colours from the temperature  $T_{eff}$  given in the table of the isochrones using following equation (e.g. Pickles et al., 1990):

$$(V - I)_C = 1512.55 - 1165.41 \log T_{eff} + 300.052 (\log T_{eff})^2 - 25.809 (\log T_{eff})^3 \quad (40)$$

For the Bolometric Correction of the V and I colours there is:

$$M_{bol} = I_C + BC_{I_C} \quad (41)$$

$$M_{bol} = V_C + BC_{V_C} \quad (42)$$

$$\implies BC_{V_C} = M_{bol} - V_C = I_C + BC_{I_C} - V_C \quad (43)$$

$$= BC_{I_C} - (V - I)_C \quad (44)$$

Bessel and Wood (1984) derived:

$$BC_{I_C} = 0.3 + 0.38(V - I)_C - 0.14(V - I)_C^2 \quad (45)$$

From Eqs. 44 and 45 follows:

$$BC_{V_C} = 0.3 - 0.62(V - I)_C - 0.14(V - I)_C^2 \quad (46)$$

Knowing  $M_{bol,iso}$  from the isochrone tables and the Bolometric Correction  $BC_{V_C}$  we calculate the visual magnitudes  $M_{V,iso}$  using Eqs. 42 and 46:

$$M_{V,iso} = M_{bol,iso} + BC_{V_C} \quad (47)$$

The mass intervals of the isochrones are fixed by their steps. The number of stars per mass interval depends on the initial mass function (IMF). This number of stars  $N_{MS}$  in a mass interval between two points of the isochrone can be calculated by (e.g. Pickles et al, 1990):

$$N_{MS} = 10^{\log \xi(\log M)} \times \Delta(\log M) \quad (48)$$

Normally we are using the IMF given by Miller & Scalo (1979) or the analytic function that has been fitted to  $\log \xi$ :

$$\log \xi(\log M) = A_0 + A_1 \log M + A_2 (\log M)^2 \quad (49)$$

But the IMF of Salpeter (1955) is incorporated in our numerical code, too.

From the number of stars per mass interval  $N_{MS}$  (Eq. 48) we calculate the total mass per interval  $M_{Tot}$ , the V light  $L_{V,Tot}$  and the bolometric light  $L_{bol,Tot}$ :

$$M_{Tot} = N_{MS} \times M \quad (50)$$

$$L_{V,Tot} = N_{MS} \times L_V \quad (51)$$

$$L_{bol,Tot} = N_{MS} \times L_{bol} \quad (52)$$

Summarising the masses and light of all  $N_{MS}$  intervals we get the total values of the individual isochrones.

Stellar spectra of the libraries have to be assigned to each point of the isochrone to construct the isochrone spectra. For each  $(V - I)_C$  colour (Eq. 40) we select from our libraries those two stars with the closest  $(V - I)_C$  colours on both sides

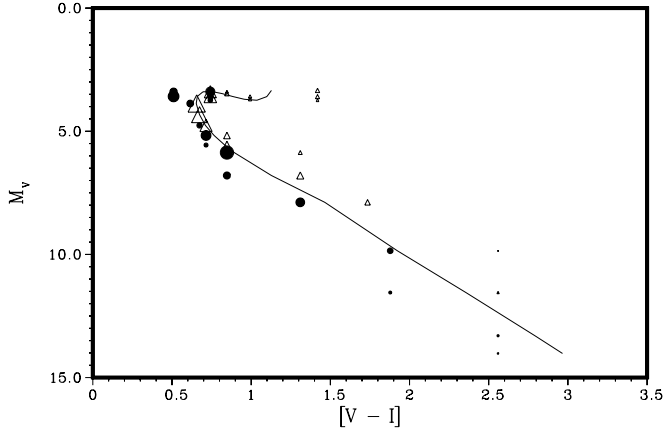


**Fig. 4.** Contribution of individual stars to construct an isochrone spectrum (age:  $6.3 \cdot 10^7$  yr)

of the isochrone regarding  $M_V$  as well. Their relative distance in the  $(V - I)_C$  colours determines the individual weight of their spectra.

Fig. 4 shows one isochrone of Bertelli et al. (1994) (age:  $6.3 \cdot 10^7$  yr) in a colour-magnitude diagram as well as symbols for the stars of the Jacoby, Hunter & Christian library we are using to construct this isochrone spectrum. The triangles represent those stars having a larger colour index  $(V - I)_C$ , the circles represent those stars having a smaller colour index in comparison to the exact values of the isochrone. The size of the symbols is proportional to the contribution of the individual stars to the final isochrone spectrum.

#### 4.1.2. Synthetic isochrone spectra from theoretical Kurucz spectra

The grid of model atmospheres of Kurucz (1994) gives us for each star the temperature  $T_{eff}$ , the gravity  $g$  and the flux  $F(\nu)$  in addition to the metallicity

We know for each isochrone of Bertelli et al. (1994) the temperature, the mass to light ratio and the partial light contribution (see Eq. 48).

Using the equations

$$L = 4\pi r^2 \sigma T_{eff}^4 \quad (53)$$

$$g = \frac{G \cdot M}{r^2} \quad (54)$$

where

(  $G$  := Gravitational constant)

(  $\sigma$  := Stefan-Boltzmann constant).

the gravity of all points of the isochrones can be determined with

$$g = \frac{M}{L} \cdot 4\pi\sigma G \cdot T_{eff}^4 \quad (55)$$

To each point of the isochrones belongs an individual gravity  $g_{iso}$  and temperature  $T_{eff,iso}$ . We assign to each point four spectra from the Kurucz library. These spectra bracket the

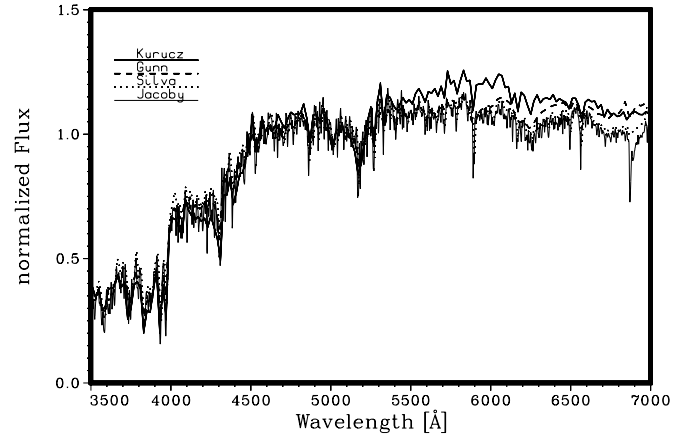


**Fig. 5.** Synthetic isochrone spectra (age:  $6.3 \cdot 10^7$  yr) constructed from different libraries

isochrone points with respect to their gravity and temperature.

We indicate them with:

$$g_+ \quad \text{for} \quad g \geq g_{iso}$$

$$g_- \quad \text{for} \quad g \leq g_{iso}$$

$$T_+ \quad \text{for} \quad T \geq T_{iso}$$

$$T_- \quad \text{for} \quad T \leq T_{iso}$$

The proportional light contribution from the individual four spectra is given by:

$$L_{\pm} = \left(1 - \frac{|T_{iso} - T_{\pm}|}{|T_+ - T_-|}\right) \cdot \left(1 - \frac{\left|\log \frac{g_{iso}}{g_{\pm}}\right|}{\left|\log \frac{g_+}{g_-}\right|}\right) \cdot L_{iso} \quad (56)$$

The masses, light and bolometric light of the isochrone points are calculated by using the Eqs. 50 to 52 described in Sect. 4.1.1.

Knowing  $F(\nu)$  we calculate the flux  $F(\lambda)$  in units of  $[erg \ s^{-1} cm^{-2} \text{\AA}^{-1}]$  of a star with radius  $r$  at a distance  $d=10$  pc by

$$F(\lambda) = 4\pi \frac{r^2}{d^2} \frac{c}{\lambda^2} \cdot F(\nu) \quad (57)$$

The final spectra of individual isochrones are determined by summing up the spectra proportional to their luminosity contribution.

#### 4.1.3. Comparison of synthetic isochrone spectra

For testing the accuracy of synthetic isochrone spectra we plot in Fig. 5 isochrone spectra for the same age ( $6.3 \cdot 10^7$  yr) and for solar metallicity but calculated with our different stellar libraries and with different methods. The spectra are normalized at  $\lambda 5050 \text{\AA}$ .

The correspondence between these spectra is quite promising. The small differences between the spectra result from differences in the spectral resolution of the stellar libraries, from the different numbers of stars in the libraries, from their completeness and from different classifications of individual stars.

There are stronger systematic differences between the observed spectral libraries and the theoretical spectra of Kurucz beyond 5500 Å. This might result from the current incompleteness of the Kurucz library with respect to cool stellar atmospheres in the temperature range from 2500 – 5000 K (Lejeune et al., 1998).

## 5. Dust extinction

First we correct all observed galaxy spectra for interstellar dust extinction from the Milky Way before starting the spectral synthesis. We estimate the galactic reddening by using the results of neutral hydrogen column density surveys (Burstein & Heiles, 1982; Hartmann & Burton, 1997).

To consider the internal extinction in the galaxies we adopt a foreground dust screen model to de-redden the stellar population. Additionally, we take into account an independent second dust screen for the central broad line region in active galaxies.

We begin our spectral syntheses of the galaxy spectra without any internal galactic reddening. Subsequently, we de-redden the observed spectra gradually and repeat the syntheses. We adopt the reddening correction that produces the minimal residuals between the synthesis spectrum and the de-reddened spectrum.

In another independent loop we de-redden the central non-thermal component. We verify this result with an additional estimation of the extinction for the broad line region derived from the Balmer decrement.

For having not too many free parameters we assume a standard galactic extinction curve (e.g. Seaton, 1979) for the de-reddening process. But extinction curves derived for the Large and Small Magellanic Clouds (Pei, 1992) are incorporated into our numerical code too.

## 6. Metallicity

The effects of various metallicities are fully included in our program code. We take into account the metallicity effects on the stellar evolutionary tracks as well as on the stellar atmospheres.

In Table 2 six different chemical compositions of our theoretical isochrones are given; they span the range from primordial abundances until solar over-abundances. With respect to the stellar libraries only the synthetic stellar spectra of Kurucz (1994) are complete for different abundances.

In practice we start our spectral syntheses with a grid of Kurucz spectra in combination with the appropriate chemical isochrone compositions. However, one shortcoming of the Kurucz stellar atmospheres is the fact that they are not complete with respect to the cool atmospheres, they do not agree completely with observed spectra (see Fig. 5) and they have a poor spectral resolution only. Therefore, we get normally smaller residuals between the synthesis models and the observed galaxy spectra when we are using the libraries with observed stellar spectra.

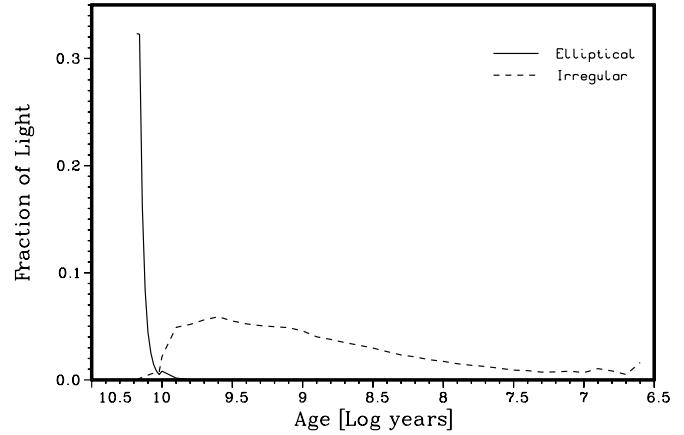


**Fig. 6.** Light contribution of individual isochrones with assumed star formation rates as function of time for an elliptical and irregular galaxy

## 7. Galaxy spectra

The spectrum of an isochrone corresponds to an accumulation of stars with all stars born at the same time. To construct a realistic galaxy spectrum with changing star formation rate within the galaxy life time we have to combine individual isochrones with different ages.

The integrated spectrum of a galaxy population with arbitrary star formation rate (SFR)  $\Psi(t)$  can be calculated by (Bruzual & Charlot, 1993):

$$F_{\lambda}(t) = \int_0^t \Psi(t - \tau) f_{\lambda}(\tau) d\tau \quad (58)$$

$f_{\lambda}(t)$  is the spectrum of an instantaneous starburst after a period of development  $t$ . The period of time that we can resolve depends on the time steps of the isochrones. Using the isochrones of Bertelli et al. (1994) we have a resolution in time of  $\sim 10^6$  to  $10^7$  years. This is sufficient to determine the long term history of galaxies.

For creating even more realistic galaxy models we can combine smoothed star formation rates with additional star forming episodes.

To carry out first test syntheses of a galaxy spectrum we made simple assumptions about the change of the star formation rate with time. Fig. 6 shows the light contribution of individual isochrones typical for an elliptical galaxy and an irregular galaxy. An exponential decreasing SFR ( $\psi = k \times e^{-t}$ ) corresponds to elliptical galaxies and an increasing SFR  $\psi = k \times t^2$  is typical for irregular galaxies (Sandage, 1986; Rocca-Volmerange & Guiderdoni, 1988).

Afterwards, we calculate theoretical spectra of these two distributions of isochrones using Kurucz library spectra with solar metallicities. Fig. 7 shows the spectra belonging to them normalized at  $\lambda 5050$  Å.

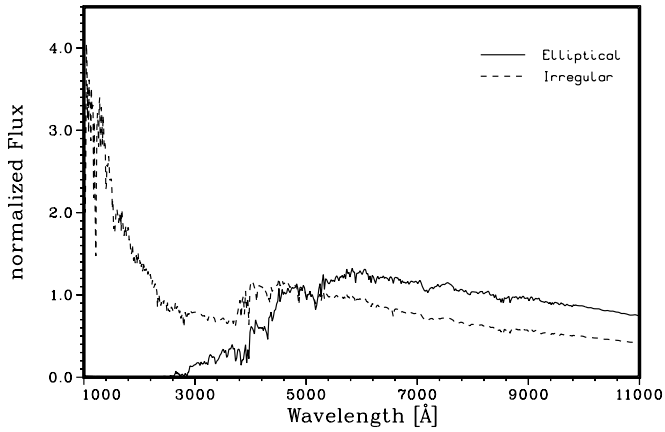


**Fig. 7.** Combined isochrone spectra corresponding to an elliptical and irregular galaxy.

### 7.1. Tests of synthetic galaxy spectra

Before starting with the synthesis of observed galaxy spectra we investigate the accuracy of our numerical method. We generate a theoretical spectrum of a 15 Gyr old elliptical galaxy with exponential decreasing SFR  $\Psi(t) \sim e^{-t}$ ; furthermore, we presume two strong starburst events took place in the galaxy  $10^8$  and  $10^9$  years ago.

The relative contribution of the individual isochrones as a function of time is plotted in Fig. 8. The accompanying optical/UV spectrum is shown in Fig. 9. Again we used the Kurucz library and the isochrones of Bertelli et al. (1994) to construct this spectrum. The spectrum has been normalized at  $\lambda 5050 \text{ \AA}$ .

Now we try to synthesize this test galaxy spectrum for which the exact stellar population and the starforming history is known with our numerical code. The calculated spectral synthesis of this test galaxy with the two starbursts is plotted over in Fig. 9. Because the synthesized spectrum is identical to the original spectrum within the width of the line no additional spectrum is to be seen. The resulting age distribution of the isochrones from this evolutionary synthesis calculation is plotted in Fig. 8 (dashed line). Again the reconstruction is almost perfect. There are only very small deviations in the very old population ( $> 10 \cdot 10^9$  years) caused by numerical errors.

This means we can reconstruct exactly the age distribution under ideal conditions with our numerical code. In practice however, our stellar libraries are to a certain amount incomplete and the isochrones are not perfect. A possible influence of reddening by dust can be overcome to a certain amount if one de-reddens the spectra. Noise contaminating observed spectra is a main problem. Therefore, we superimposed noise to the test spectrum. We added Gaussian noise of 3% relative intensity to the test spectrum. This corresponds to an upper limit in the S/N ratio for reliability and uniqueness on the information content of the data (e.g. O'Connell, 1996). Fig. 10 shows this spectrum.

Afterwards, we repeated the evolutionary synthesis of the test spectrum with noise superimposed. The new synthesized spectrum is plotted over the test spectrum in Fig. 10. Differences between these two spectra result mainly from the noise in the

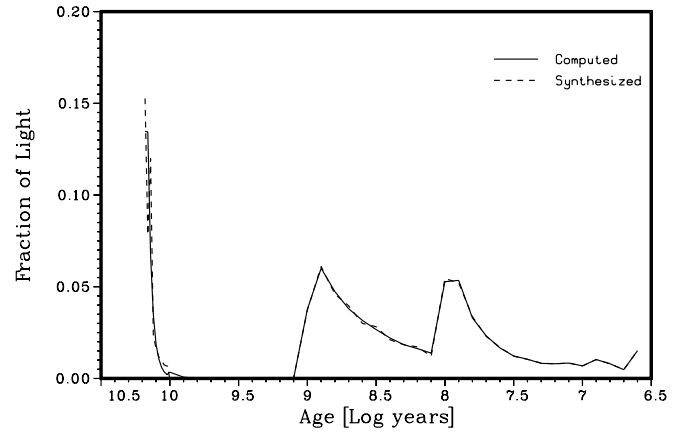


**Fig. 8.** Assumed and reconstructed (dashed) age distribution of the isochrones of an elliptical galaxy undergone two starburst events  $10^8$  and  $10^9$  years ago.

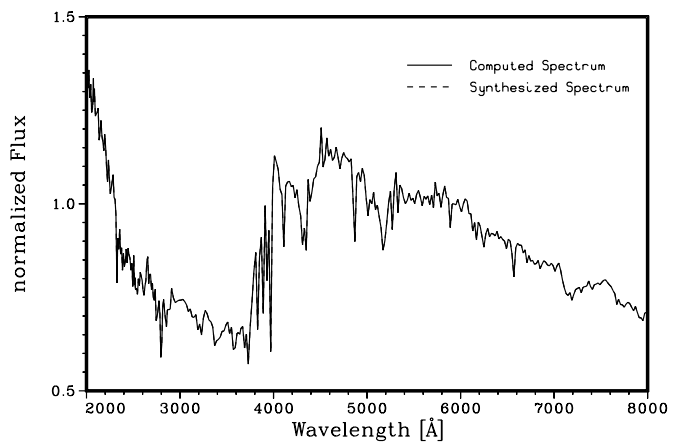


**Fig. 9.** Computed and reconstructed (dashed) spectra of an elliptical galaxy undergone two starburst events  $10^8$  and  $10^9$  years ago.

test spectrum. The synthesized spectrum corresponds to a galaxy spectrum without noise.

The result of our evolutionary synthesis is shown in Fig. 11. The age distribution of the isochrones (dashed line) is plotted together with the initially assumed distribution. The basic pattern of both curves is equal. There is an old stellar population ( $> 10 \cdot 10^9$  yr) with two starburst components of roughly the correct age  $10^8$  and  $10^9$  years ago. The share of the integrated light fractions of both starbursts is equal within 20 percent. The moment of both starburst events is correct within 10 percent. This example demonstrates that high quality spectra are suitable for a detailed analysis.

### 7.2. Spectral synthesis of the elliptical galaxy NGC 4476

An optical spectrum of the dwarf elliptical galaxy NGC 4476 has been obtained by Bica (1988). Details of the observation and reduction methods are to be found there. Arimoto (1996) distributed this spectrum world wide for a contest of population

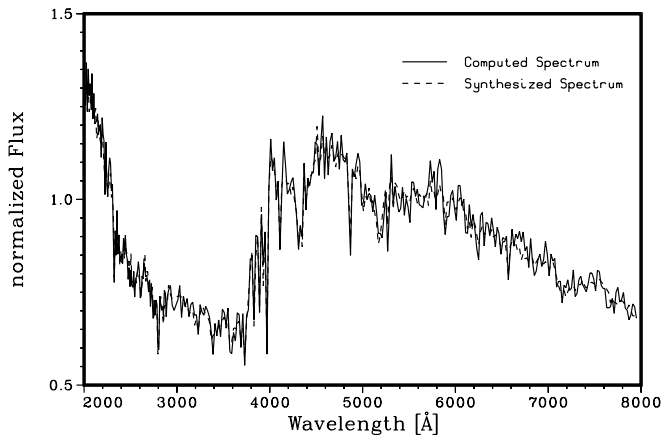


**Fig. 10.** Galaxy test spectrum with noise superimposed and synthesized spectrum

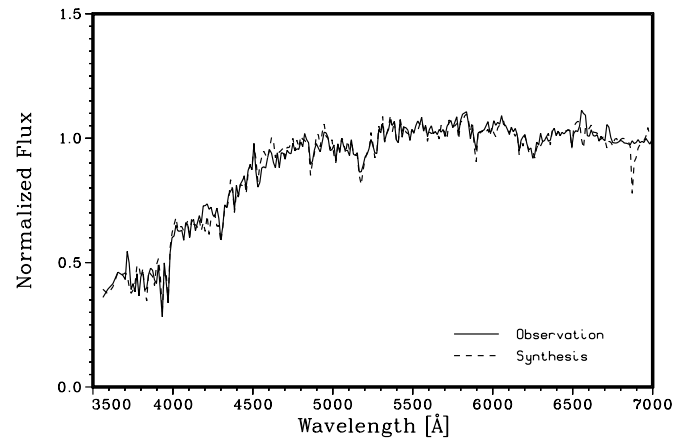


**Fig. 12.** Observed and synthesized (dashed) spectrum of the elliptical galaxy NGC 4476

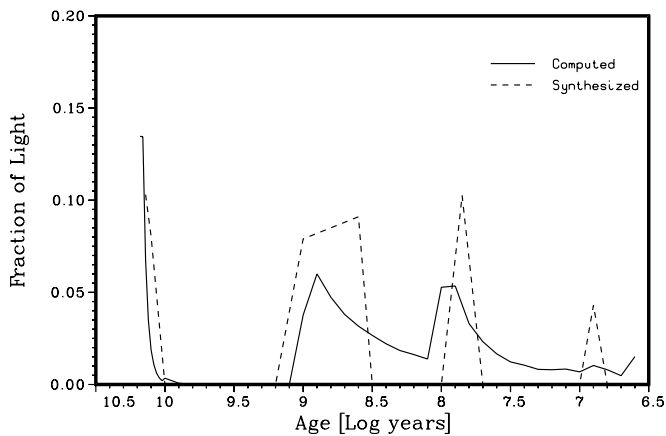


**Fig. 11.** Assumed and reconstructed age distribution of the isochrones of our test galaxy with superimposed noise.

synthesis models. Fig. 12 shows the distributed optical spectrum and our synthesis with isochrone spectra.

We performed the evolutionary synthesis calculations with the Bertelli et al. (1994) isochrones and with the four stellar libraries described in Sect. 2. When using the Kurucz library we got systematic deviations in our spectral fits. This was caused mainly by the incompleteness of this library with respect to cooler stellar atmospheres. We obtained our best results when we used the Jacoby, Hunter & Christian library. This is the most complete library and has the best spectral resolution in comparison to the others. Furthermore, we received the best fit without any internal reddening in this elliptical galaxy.

We calculated a dominant old component of 16 Gyr (75%), a component of around 10 Gyr (20%) and a weak 'young' component of 1 Gyr (5%). The weak emission lines of  $H\alpha$  and [SII] confirm the existence of a young component too in this elliptical galaxy.

Our results were in good accordance with other optimizing synthesis models (Arimoto, 1996).

### 7.3. Spectral synthesis of the Seyfert galaxy NGC 1365

Recent models of active galactic nuclei (e.g. Shlosman et al., 1989) predict nuclear starbursts and/or central non-thermal activities forced by instabilities of the in-flowing gas due to tidal interactions. On the other hand the UV- and X-rays coming from the (non-thermal) nucleus may interact with the ISM leading to substantial star formation. Therefore, the stellar composition in active galaxies is an important tool to test these models.

NGC 1365 is a bright, nearby Seyfert 1 galaxy of Hubble type SBb. We carried out spectroscopic observations of NGC 1365 with the ESO 2.2m telescope. We used a CCD-camera with a RCA chip attached to the Boller&Chivens spectrograph. A slit width of 2.5 arcsec was used under seeing conditions of 1.5 arcsec. We oriented the slit in north-south direction. We took spectra with exposure times of 2 x 40 min for the blue spectral range (3700 – 5440 Å) and 2 x 30 min for the red spectral range (5250 – 7000 Å). The spectral resolution was  $\sim 4$  Å. Calibration and reduction of the data was done in the usual way (e.g. Kollatschny et al., 1992). The spatial resolution of our spectra amounts to 2-3 arcsec corresponding to 0.2 – 0.3 kpc at the distance of the galaxy. After reduction we divided the spatially resolved long-slit spectra into individual intervals. Spectra and syntheses of the nuclear region in NGC 1365 and of two outer regions at distances of 1 kpc and 3 kpc are presented in this paper. The spectra of the inner regions were integrated over  $3 \times 2.5$  arcsec. For improving the signal-to-noise ratio we integrated over  $6 \times 2.5$  arcsec at 3 kpc distance from the center. The observed spectra are shown in Figs. 13 to 15.

Again we carried out the spectral synthesis with the Bertelli isochrones and all libraries. The emission line regions in the spectra were eliminated by zero weighting during the syntheses. As it was the case for the elliptical galaxy NGC 4476 we received the best results with the Jacoby, Hunter & Christian library. The spectral syntheses are plotted over the observed spectra in Figs. 13 to 15.

One can see that spectral syntheses are important for the exact measurement of the true emission line intensities in the

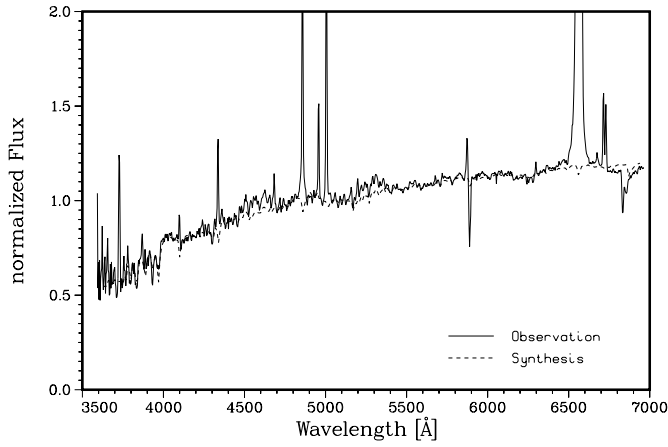


Fig. 13. Observed and synthesized nuclear spectrum of NGC 1365

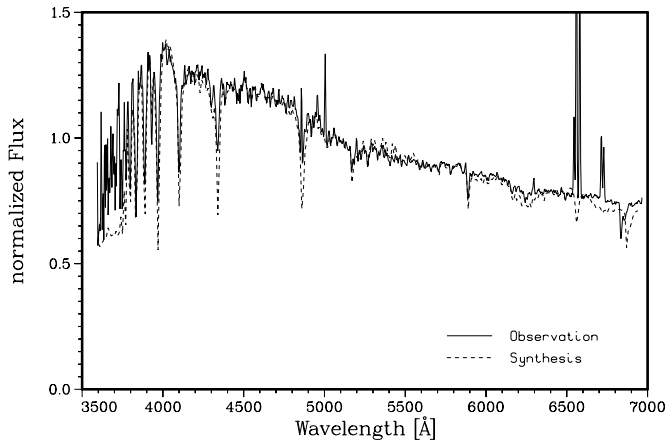


Fig. 14. Observed and synthesized spectrum at 1 kpc distance from center of NGC 1365

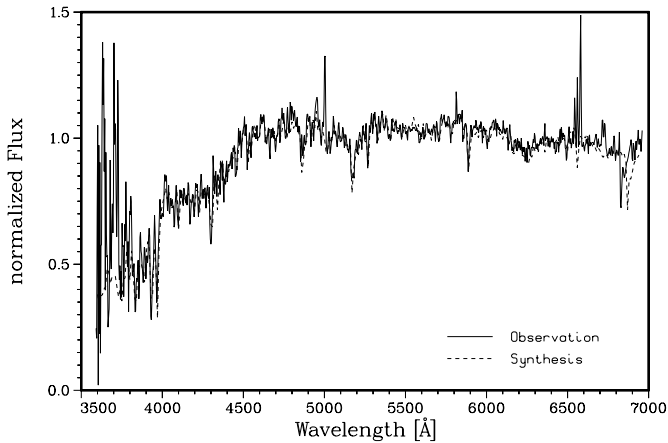


Fig. 15. Observed and synthesized spectrum at 3 kpc distance from center of NGC 1365

case of the Seyfert spectrum of NGC 1365 (Fig. 13). The intensity of e.g. the FeII blends at  $\lambda\lambda$  4450–4800, 5080–5400  $\text{\AA}$  can be determined more reliable. Sometimes the emission lines are heavily blended with absorption lines (e.g.  $H\beta$ ,  $H\gamma$  in Fig. 14). The knowledge of the underlying absorption spectrum

**Table 3.** Light fraction of important isochrones (normalized at  $\lambda 5050 \text{ \AA}$ ) of three regions in the Seyfert galaxy NGC 1365.

age [yr]	center	1 kpc	3 kpc
$> 3 \cdot 10^9$	70	30	54
$1-3 \cdot 10^9$	–	–	45
$10^8 - 10^9$	9	1	1
$< 10^8$	21	69	–

is of great importance for deriving the Balmer decrement and performing reddening corrections of the emission lines.

Results of the evolutionary syntheses of three regions in NGC 1365 are tabulated in Table 3.

The stellar light fraction of the central Seyfert spectrum has been normalized to 100 percent after subtraction of the share of the non-thermal component for comparison of the different regions. In Table 3 only the dominant components are listed having a fraction of light larger than 1 percent.

The nuclear spectral component is dominated by a non-thermal component. Its light contribution amounts to 60 percent at  $\lambda 5050 \text{ \AA}$ . Furthermore, we received the best result with an extinction  $E_{(B-V)} = 0.4$  for the non-thermal component. Only in the nuclear spectrum we got a better result with the addition of a non-thermal component. This was not the case for the outer regions. The contribution of the FeII quasi continuum amounted to 0.2 percent in the nuclear spectrum.

For fitting the spectra we had to consider an extinction of the intrinsic stellar component too. The extinction was strongest at the nuclear region ( $E_{(B-V)} = 0.29$ ) and decreased towards the outer regions (3–9 kpc away from the center) to values of  $E_{(B-V)} = 0.1 - 0.05$ .

There is a strong young ( $< 10^8$  yr) stellar component at the nuclear region of NGC 1365. But at a distance of 1 kpc there is an even stronger starburst region. This component might be connected to the barred structure of this galaxy. Bars can drive much of the internal galactic gas to the inner hundreds of parsecs of a galaxy leading to star forming activities (e.g. Phinney, 1994). Only a smaller amount of gas might be driven to the central tens of parsecs by a secondary bar (Shlosman et al., 1989).

Our synthesis example shows that the contribution of a non-thermal component can be of great importance for the spectral analysis of active galactic nuclei. In a forthcoming paper we will investigate in detail the contribution of a central non-thermal component in the optical and correlate this result with other activity as well as starburst properties in AGN spectra.

## 8. Conclusion

We have presented our new numerical code to perform population and evolutionary syntheses of galaxy spectra. Our modified simplex algorithm leading towards the unique optimal solution has the advantage that no initial solution is required, the non-negativity for the individual contributions is guaranteed, addi-

tional spectral components can be added and individual wavelength regions can be weighted. We demonstrated the accuracy of our method presenting syntheses of artificial spectra. The ability of our numerical code was demonstrated for spectra of an elliptical galaxy and spatially resolved spectra of the Seyfert galaxy NGC 1365.

In a second paper we will present applications of our numerical method on long-slit spectra of a large sample of nearby active galaxies.

*Acknowledgements.* This work has been supported by the Deutsche Forschungsgemeinschaft Ko 857/14-1/2

## References

- Arimoto N., 1996, In: From Stars To Galaxies, ASP Conf. Series 98, Leitherer C. et al.(ed), p.287
- Arimoto N., Yoshii Y., 1987, A&A 173, 23
- Bertelli G., Bressan A., Chiosi C., Fagotto F., Nasi E., 1994, A&AS 106, 275
- Bessel M.S., Wood P.R., 1984, PASP 96, 247
- Bica E., 1988, A&A 195, 76
- Bica E., Alloin D., 1986, A&A 162, 21
- Bruzual G.A., 1983, ApJ 273, 105
- Bruzual G.A., Charlot S., 1993, ApJ 405, 538
- Burstein D., Heiles C., 1982, AJ 87, 1165
- Goerdt A., Kollatschny W., 1996, In: From Stars To Galaxies', ASP Conf.Series 98, Leitherer C. et al.(ed.), p.521
- Guiderdoni B., Rocca-Volmerange B., 1987, A&A 186, 1
- Gunn J.E., Stryker L.L., 1983, ApJS, 52, 121
- Hadley G., 1962, In:Linear Programming, Addison-Wesley, Reading, MA
- Hartmann D., Burton W.B., 1997, in 'Atlas of Galactic Neutral Hydrogen', Cambridge Univ. Press
- Jacoby G.H., Hunter D.A., Christian, C.A., 1984, ApJS 56, 257
- Kollatschny W., Dietrich M., Hagen H., 1992, A&A 264, L5
- Kollatschny W., Goerdt A., 1997, In Proc. of the ESO Workshop: The Early Universe with the VLT, Bergeron J.(ed), p.400
- Kollatschny W., Goerdt A., 1998, In: The Central Regions of the Galaxy and Galaxies, Sofue Y. et al.(ed), IAU Symp.184, Kyoto (in press)
- Kurucz R., 1992, In: The Stellar Populations of Galaxies, Barbuy B., Renzini A. (eds.), IAU Symp.149, Dordrecht, Kluwer, p.225
- Kurucz R., 1994, private communication
- Lejeune T., Cuisinier F., Buser R., 1998, A&A (in press)
- Miller G.E., Scalo J.M., 1979, ApJS 41, 513
- Netzer H., Wills B.J., 1983, ApJ 275, 445
- O'Connell R.W., 1976, ApJ 206, 370
- O'Connell R.W., 1996, In: From Stars To Galaxies, ASP Conf.Series 98, Leitherer C. et al. (ed), p.3
- Pei Y.C., 1992, ApJ 395, 130
- Pelat D., 1997, MNRAS 284, 365
- Phinney E.S., 1994, In: Mass-Transfer Induced Activity in Galaxies, Shlosman I. (ed.), Cambridge Univ. Press, p.1
- Pickles A.J., van der Kruit P.C., 1990, A&AS 84, 421
- Rocca-Volmerange B., Guiderdoni B., 1988, A&AS 75, 93
- Salpeter E.E., 1955, ApJ 121, 161
- Sandage A., 1986, A&A 161, 89
- Seaton M.J., 1979, MNRAS 187, 73P
- Shlosman I., Frank J., Begelman M.C., 1989, Nat 338, 45
- Silva D.R., Cornell M.E., 1992, ApJS 81, 865
- Wills B.J., Netzer H., Wills D., 1985, ApJ 288, 94